

Big EEG Data Images for Convolutional Neural Networks

S. Thundiyil¹, M. Thungamani², S.A. Hariprasad³

1. Department of ECE, BMS Institute of Technology and Management, Bangalore, India
2. Department of Computer Science, CoH, University of Horticultural Sciences, Bangalore, India
3. Faculty of Engineering and Technology, Jain Deemed to be University, Bangalore, India
saneesh@bmsit.in, thungamani_k@rediffmail.com, sa.hariprasad@jainuniversity.ac.in

An open image database of Electroencephalogram (EEG) plays a vital role in developing deep learning algorithms for conducting research in EEG signal processing. This abstract presents the generation of “Big EEG Data” images for researchers to develop and test deep learning algorithms, especially using convolutional neural networks. The image database created in this work uses the Temple University Hospital (TUH) Electroencephalography Seizure Corpus (TUSZ) [1]. We have used ‘TUSZ v1.5.2’ database for the creation of the images [2].

An EEG signal in its general form is considered as a time series data where the temporal information and spectral information play a crucial role in understanding the underlying characteristics of the signal. There are several deep learning techniques proposed for the analysis and classification of time series data. Apart from the prominent architectures in recurrent neural networks, researchers propose novel algorithms to address time-series data classification and prediction issues [3]–[5]. The studies suggested by Lotte et al. [6] reveal that the researchers are applying deep learning methodologies to detect and classify epileptic seizures. However, there is a need to improve the accuracy. Convolutional neural networks are very well matured to classify images into multiple classes. In this work, we propose to use the convolutional neural networks for the classification of EEG signals. The challenges here are the time series representation of the EEG signal itself. It may be noted that standard time-series deep learning architectures such as LSTM, RNN, etc., can work directly on the time series data, whereas CNN cannot be directly used on such data. Hence, we suggest converting the EEG signal to a set of images by extracting three characteristics of time-sliced EEG signals. The methods proposed in this abstract do not directly represent EEG time-domain signal in the image format, but the image representation of the values obtained while performing three transformation techniques as explained below.

The conversion of time-series data such as EEG into an image is performed by obtaining properties such as mutual information and correlation between a set of successive samples in EEG signals and by obtaining the discrete cosine transform and hence spectrogram of EEG signals. Obtaining the mutual information and correlation coefficient values are done after converting the EEG signal of long duration into short-duration signals through time slicing based on ECG rhythms.

The methodology adopted to convert the time series data into images is illustrated in Figure 1. The steps involved in the creation of an image database are:

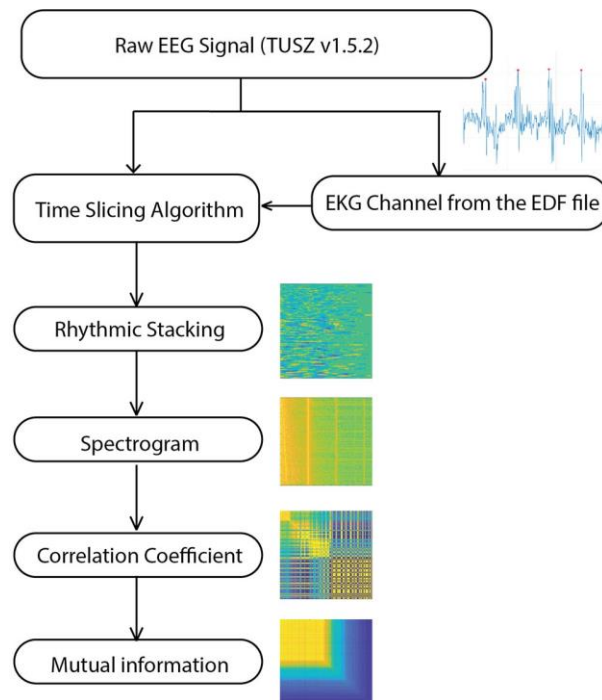


Figure 1. Block diagram of the methodology adopted

1. Time-slicing of EEG data based on ECG rhythms;
2. EEG image creation using rhythmic stacking;
3. Images based on mutual information available in the successive block samples;
4. Images based correlation information of time slices;
5. Images based on spectrogram information of time slices.

The underlying principle of our approach is the time-slicing of the EEG recordings based on the R peaks of the ECG signal. Different studies by Ako.M et al. [7] and Bhavsar et al. [8] provide an insight into the correlation between EEG activities and heart rate variability. Hence a time-slicing approach based on '*r peaks*' was chosen to study the EEG patterns. The first algorithm makes the simple stacking of EEG patterns based on the ECG rhythms. The EEG recording available in the TUH Seizure Corpus is in the European data format (edf). Most of the recordings in this corpus contain 21-32 channels per recording. In our algorithm, we have separated the ECG channel by extracting the label EKG-REF or equivalent label from '*edf*' file. Later the sample index corresponding to '*r peaks*' was obtained after finding the peaks. Since the time duration of all the channels is the same for one recording, we have sliced the EEG channels based on the '*r peaks*' of the ECG waveform. Each such slice is now stacked together to form image data. The slicing procedure and sample of a resultant image is shown in Figure 2. To make the size (width) of the image the same, we introduced zero padding if there is a mismatch in the length of each segment due to variation in R-R interval.

In the second algorithm, we used the entire channel recording without time slicing to obtain the spectrogram images. We use one image for each channel as indicated in Figure 3(a). The spectrogram uses the Short Time Fourier Transform, which is a useful transformation technique since it preserves both time and frequency domain characteristics [9]. The total number of images generated is based on the number of channels available in each '*edf*' file.

In the third algorithm, the correlation coefficient between each time-sliced segment was obtained. Cross-correlation is a technique that estimates the correlation between two signals. Cross-correlation accounts for time delays by shifting one of the two signals [10]. In our approach, the correlation is calculated between two slices, and a matrix is created using the correlation values between each slice. Hence for one channel,

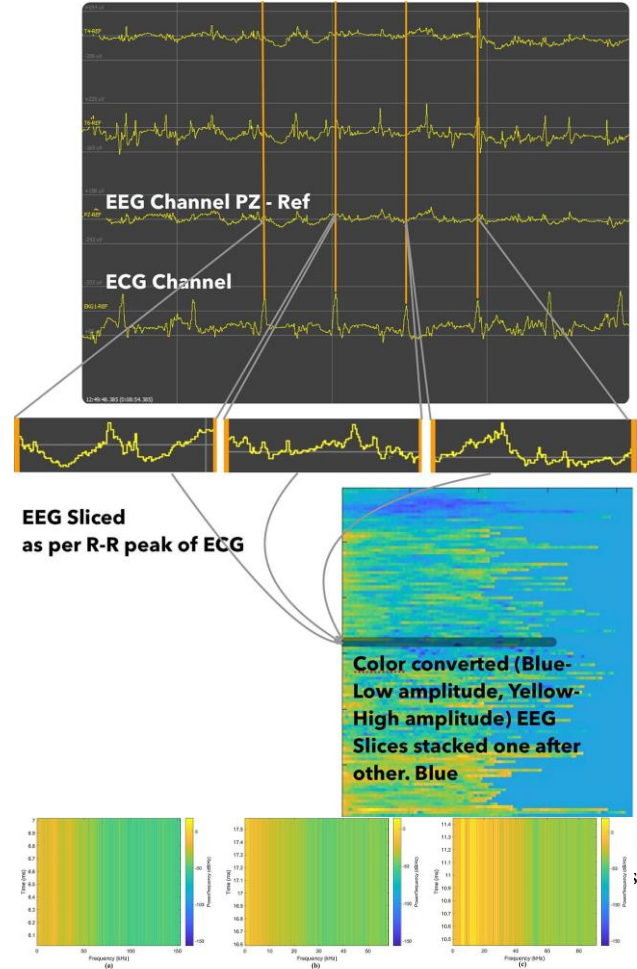


Figure 3(a). Sample images of spectrogram of entire channel

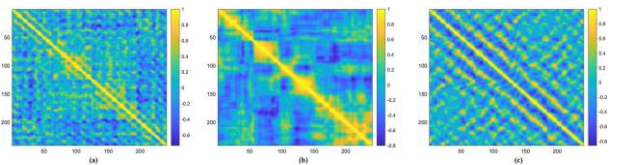


Figure 3(b). Sample images based on correlation coefficient between every EEG slices

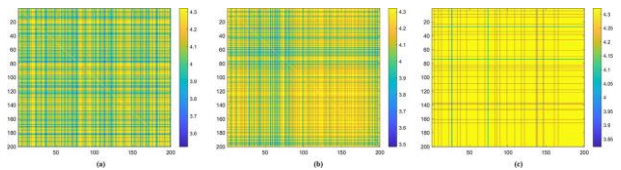


Figure 3(c). Sample images based on mutual information between every EEG slices

if the number of slices is M , we get M correlation coefficient values for each slice. We get a total of $M \times M$ matrix of correlation coefficients. This matrix is further converted to image format. Hence for each recording, we got the number of images equivalent to the number of EEG channels. Similarly, in the fourth algorithm, the mutual information between every slice of each channel is obtained [11]. The mutual information matrix corresponds to each channel is converted to images. Figure 3(b) and Figure 3(c) shows the sample images generated using correlation coefficient and mutual information based algorithms.

All the images obtained from these four algorithms have the same naming conventions as indicated in Figure 4 except for the algorithm name field. We have used complete TUEZ v1.5.2 resources for the creation of two master databases. In the first database, all the images were formed by implementing all four algorithms to entire EEG recordings irrespective of the seizure occurrence. The second database is created by implementing all four algorithms to the portion of the recording where seizure is identified. This was done by extracting the starting and ending time of occurrence of seizure. The details about the time record are provided in the documentation available in the TUSZ corpus.

The number of images generated against each category is indicated in Table 1. The images created are categorically saved to different folders, corresponding to eight different classes, as shown in Table 2. The top-level folder contains the training and development folders named exactly as per the TUSZ naming conventions. Each of these folders has four subfolders which is named based on the image creation method adopted, such as Stacked, Spectrogram, Cross_Correlation, and Mutual_Information. Each of these folders contains seven subfolders which is named as per Table 2. Each of these folders is a seizure class. The typical filename in each of these folders is in the format as mentioned in Figure 4. The patient number, session ID, and session number fields are the same as in the original EEG file available in the EDF format in the TUSZ database. Using the same naming convention makes it easy for researchers to compare the deep learning algorithms with works that

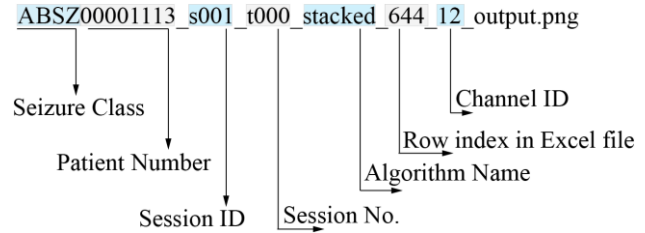


Figure 4. Description of filename

Table 1. Number of images generated under various classes

	Seizure Category	Stacked images		Spectrogram Images		Correlation based images		Mutual information-based images	
		Train	Dev	Train	Dev	Train	Dev	Train	Dev
Image Data Bank 1	FNSZ	26179	2286	42577	4679	2627	1029	232	32
	GNSZ	6415	1644	10964	1592	356	438	121	104
	SPSZ	1179	96	1298	93	151	130	92	34
	CPSZ	4119	256	8797	1111	488	258	164	117
	ABSZ	1056	192	1573	192	84	100	257	111
	TNSZ	279	95	486	589	248	498	215	99
	TCSZ	494	409	900	506	273	348	278	101
	MYSZ	64	32	64	32	64	32	125	10
	Total	39785	5010	66659	8794	4291	2833	1484	608
Image Data Bank 2	FNSZ	1600	1568	672	1568	1582	-	704	-
	GNSZ	7250	2680	6416	2622	3001	-	526	-
	SPSZ	38155	9156	38565	8787	32515	-	950	-
	CPSZ	11199	4880	9052	4751	7741	-	786	-
	ABSZ	64	-	-	32	64	-	64	-
	TNSZ	1462	96	1277	93	1433	-	117	-
	TCSZ	907	550	420	537	907	-	315	-
	MYSZ	540	1408	485	1364	540	-	247	-
	Total	61177	20338	56887	19754	47783	0	3709	0

Table 2. Folder names corresponds to each class

Folder Name	Event Name
FNSZ	Focal Non-Specific Seizure
GNSZ	Generalized Non-Specific Seizure
SPSZ	Simple Partial Seizure
CPSZ	Complex Partial Seizure
ABSZ	Absence Seizure
TNSZ	Tonic Seizure
TCSZ	Tonic Clonic Seizure
MYSZ	Myoclonic Seizure

Table 3. Training options selected for Alexnet architecture

Solver	sgdm
Initial learning rate	0.0001
Validation frequency	50
Epochs	30
Minimum batch size	128
L ₂ Regularization	0.0001
Gradient Threshold	L ₂ Norm
Method	
Momentum	0.9

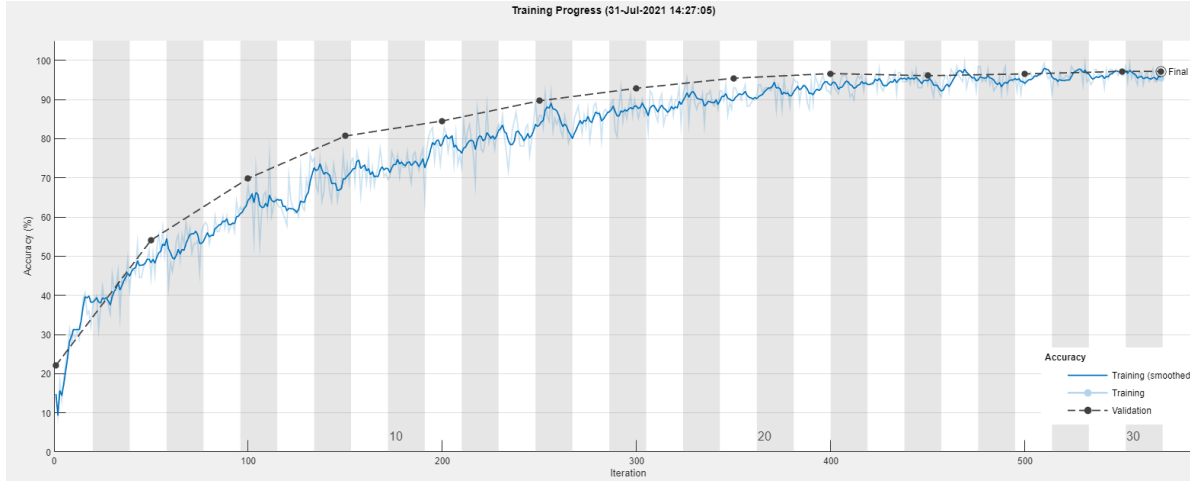


Figure 5. Training Progress of mutual information based images with AlexNet architecture

directly use the TUSZ data. The images are cropped to remove the axis information which is generated while implementing the algorithms.

Authors have tested these images for classification accuracy using convolutional neural networks architectures. Since images pertaining to each class is available in separate folders, standard Alexnet architecture, Resnet18 architecture, and GoogleNet architecture were used for testing the classification accuracy [12][13]. We have implemented the architecture for multiclass problems (7-Class) by changing parameters in the fully connected layer of CNN architecture, such as the number of output classes. As indicated in Table 1, the number of images per class is not balanced. This is due to the insufficient recordings available in the corpus for a particular type of seizure (e.g., Myoclonic Seizure). Due to the imbalance in the data, other than validation accuracy, we have calculated F1-Score and Specificity. The values of training options (hyperparameters) used for training the Alexnet architecture are listed in Table 3. Similar training options were provided for the other two architectures as well. Figure 5 shows the training progress upon training Alexnet architecture with mutual information based images. The confusion matrix obtained for the same database (mutual information based images) are shown in Figure 6. Similarly, all four image databases were tested with three CNN architectures. The results obtained in each case are tabulated in Table 4.

The performance of these methods is compared with similar works performed on the TUH database by other authors. Golmohammadi et al. used gated recurrent units (CNN/GRU) and LSTM models on TUH Seizure data for

		Confusion Matrix						
Output Class	ABSZ	207 19.0%	1 0.1%	0 0.0%	1 0.1%	0 0.0%	0 0.0%	99.0% 1.0%
	CPSZ	0 0.0%	153 14.0%	1 0.1%	0 0.0%	0 0.0%	0 0.0%	99.4% 0.6%
	FNSZ	0 0.0%	0 0.0%	277 25.4%	6 0.5%	0 0.0%	0 0.0%	97.2% 2.8%
	GNSZ	4 0.4%	3 0.3%	4 0.4%	229 21.0%	0 0.0%	0 0.0%	95.4% 4.6%
	SPSZ	0 0.0%	0 0.0%	0 0.0%	0 0.0%	33 3.0%	1 0.1%	97.1% 2.9%
	TCSZ	0 0.0%	1 0.1%	1 0.1%	0 0.0%	0 0.0%	91 8.3%	97.8% 2.2%
	TNSZ	0 0.0%	0 0.0%	2 0.2%	0 0.0%	2 0.2%	70 6.4%	92.1% 7.9%
		98.1% 1.9%	96.8% 3.2%	97.2% 2.8%	97.0% 3.0%	94.3% 5.7%	96.8% 3.2%	97.2% 2.8%
		Target Class						
		ABSZ	CPSZ	FNSZ	GNSZ	SPSZ	TCSZ	TNSZ

Figure 6. Confusion matrix for mutual information image based classification

Table 4. Performance parameters

Spectrogram Images (AlexNet)	F1 - Score	97.47
	Accuracy	97.15
	Specificity	99.51
Correlation Coefficient based Images (ResNet-18)	F1 - Score	93.64
	Accuracy	93.45
	Specificity	98.88
Mutual information based Images (ResNet-18)	F1 - Score	97.95
	Accuracy	97.89
	Specificity	99.62
Stacked Images (ResNet-18)	F1 - Score	95.64
	Accuracy	95.50
	Specificity	99.24

classification and achieved specificity of 97.1 % and 91.49 %, respectively [14]. L. Wei and A. Mooney presented the XGBoost-based method to detect seizures from TUH Corpus. They have achieved an accuracy of 67.01% while training and 58.85% during validation [15]. For the abnormal dataset from the TUH EEG corpus, S Roy et al. applied 1D-CNN-RNN and could achieve an accuracy of 82.27% [16]. Yildirim et al. proposed a 1D CNN model to classify the normal and abnormal EEG signal from the TUH EEG corpus and achieved an F1-Score of 78.92 and an accuracy of 79.34% [17]. In several performance parameters, our proposed methods have shown better results for the training dataset.

In this abstract, we have discussed the generation of an image database from TUSZ v1.5.2 using four techniques. The EEG time-domain signal extracted from the 'edf' file is converted into images based on four properties of the time-sliced EEG signal. The image database is tested for classification accuracy using convolutional neural networks. The highest accuracy of 97.89% has been achieved when trained ResNet architecture with images based on mutual information. The accuracy achieved is for seven classes. The image database serves as a valuable resource for training deep learning networks.

REFERENCES

- [1] A. Harati, S. Lopez, I. Obeid, J. Picone, M. P. Jacobson, and S. Tobochnik, "The TUH EEG CORPUS: A big data resource for automated EEG interpretation," in *Proceedings of the IEEE Signal Processing in Medicine and Biology Symposium (SPMB)*, Dec. 2015, pp. 1–5, doi: 10.1109/spmb.2014.7002953.
- [2] V. Shah *et al.*, "The Temple University Hospital Seizure Detection Corpus," *Front. Neuroinform.*, vol. 12, p. 83, 2018, doi: 10.3389/fninf.2018.00083.
- [3] P. Lara-Benitez, M. Carranza-Garcia, and J. C. Riquelme, "An Experimental Review on Deep Learning Architectures for Time Series Forecasting," *International Journal of Neural Systems*, vol. 31, no. 3, p. 213001, 2021, doi: 10.1142/S0129065721300011.
- [4] Gamboa, John Cristian Borges. "Deep learning for time-series analysis," 2017, *arXiv preprint*, arXiv: 1701.01887.
- [5] H. I. Fawaz, G. Forestier, J. Weber, L. Idoumghar, and P.-A. Muller, "Deep learning for time series classification: a review," *Data Min. Knowl. Discov.*, vol. 33, no. 4, pp. 917–963, 2019, doi: 10.1007/s10618-019-00619-1.
- [6] Lotte, Fabien, et al. "A review of classification algorithms for EEG-based brain–computer interfaces: a 10 year update," *Journal of Neural Engineering* 15.3, 2018, 031005, doi: 10.1088/1741-2552/aab2f2.
- [7] M. Ako *et al.*, "Correlation between electroencephalography and heart rate variability during sleep," *Psychiatry Clin. Neurosci.*, vol. 57, no. 1, p. 59–65, Feb. 2003, doi: 10.1046/j.1440-1819.2003.01080.x.
- [8] R. P. Bhavsar, "Assessing variability of EEG and ECG/HRV time series signals using a variety of non-linear methods," University of Hertfordshire, 2020, doi: 10.18745/th.22617.
- [9] Y. Yuan, G. Xun, K. Jia, and A. Zhang, "A multi-view deep learning framework for EEG seizure detection," *IEEE J. Biomed. Heal. Informatics*, vol. 23, no. 1, pp. 83–94, 2019, doi:10.1109/jbhi.2018.2871678.
- [10] Tsiouris KM, Pezoulas VC, Zervakis M, Konitsiotis S, Koutsouris DD, Fotiadis DI. A Long Short-Term Memory deep learning network for the prediction of epileptic seizures using EEG signals. *Comput Biol Med.* Aug 2018,vol. 99, pp. 24-37. doi: 10.1016/j.combiomed.2018.05.019.
- [11] Ince, Robin AA, et al. "A statistical framework for neuroimaging data analysis based on mutual information estimated via a gaussian copula," *Human brain mapping* 38.3, 2017, 1541-1573, doi:

10.1002/hbm.23471.

- [12] A. Krizhevsky, I. Sutskever, and G. E. Hinton, "Imagenet classification with deep convolutional neural networks," in *Advances in Neural Information Processing Systems*, 2012, pp. 1097–1105. Available: <https://dl.acm.org/doi/10.5555/2999134.2999257>.
- [13] K. He, X. Zhang, S. Ren and J. Sun, "Deep Residual Learning for Image Recognition," *2016 IEEE Conference on Computer Vision and Pattern Recognition (CVPR)*, 2016, pp. 770-778, doi: 10.1109/CVPR.2016.90.
- [14] M. Golmohammadi *et al.*, "Gated recurrent networks for seizure detection," *2017 IEEE Signal Processing in Medicine and Biology Symposium (SPMB)*, 2017, pp. 1-5, doi: 10.1109/SPMB.2017.8257020.
- [15] L. Wei and C. Mooney, "Epileptic Seizure Detection in Clinical EEGs Using an XGboost-based Method," in *2020 IEEE Signal Processing in Medicine and Biology Symposium (SPMB)*, 2020, pp. 1–6, doi: 10.1109/SPMB50085.2020.9353625.
- [16] S. Roy, I. Kiral-Kornek, and S. Harrer, "Deep Learning Enabled Automatic Abnormal EEG Identification," in *2018 40th Annual International Conference of the IEEE Engineering in Medicine and Biology Society (EMBC)*, 2018, pp. 2756–2759, doi: 10.1109/EMBC.2018.8512756.
- [17] Ö. Yildirim, U. B. Baloglu, and U. R. Acharya, "A deep convolutional neural network model for automated identification of abnormal EEG signals," *Neural Comput. Appl.*, pp. 1–12, 2018, doi: 10.1007/S00521-018-3889-Z.

Big EEG Data Images for Convolutional Neural Networks

S. Thundiyl¹, M. Thungamani², S.A. Hariprasad³

1. Department of ECE, BMS Institute of Technology and Management, Bangalore, India
2. Department of Computer Science, CoH, University of Horticultural Sciences, Bangalore, India
3. Faculty of Engineering and Technology, Jain Deemed to be University, Bangalore, India

ABSTRACT

- An open image database of Electroencephalogram (EEG) plays a vital role in developing deep learning algorithms for conducting research in EEG signal processing.
- This abstract presents the generation of “Big EEG Data” images for researchers to develop and test deep learning algorithms, especially using convolutional neural networks.
- The image database created in this work uses the Temple University Hospital (TUH) Electroencephalography Seizure Corpus (TUSZ). We have used ‘TUSZ v1.5.2’ database for the creation of the images.

NEED OF IMAGE REPRESENTATION

- An EEG signal is generally represented as a time-domain. The temporal information and spectral information play a crucial role in understanding the underlying characteristics of the signal.
- It may be noted that standard time-series deep learning architectures such as LSTM, RNN, etc., can work directly on the time series data.
- Convolutional neural networks are very well matured to classify images into multiple classes. In this work, we propose to use the convolutional neural networks directly for the classification of EEG signals. The challenge is that CNN cannot be used on time series data.
- We suggest converting the EEG signal to a set of images by extracting three characteristics of time-sliced EEG signals.

TIME SERIES TO IMAGES

- The conversion of time-series data such as EEG into an image is performed by obtaining properties such as mutual information and correlation between a set of successive samples in EEG signals and by getting the discrete cosine transform and hence spectrogram of EEG signals. Obtaining the mutual information and correlation coefficient values are done after converting the EEG signal of long duration into short-duration signals through time slicing based on ECG rhythms.
- The methodology adopted to convert the time series data into images is illustrated in Figure 1.

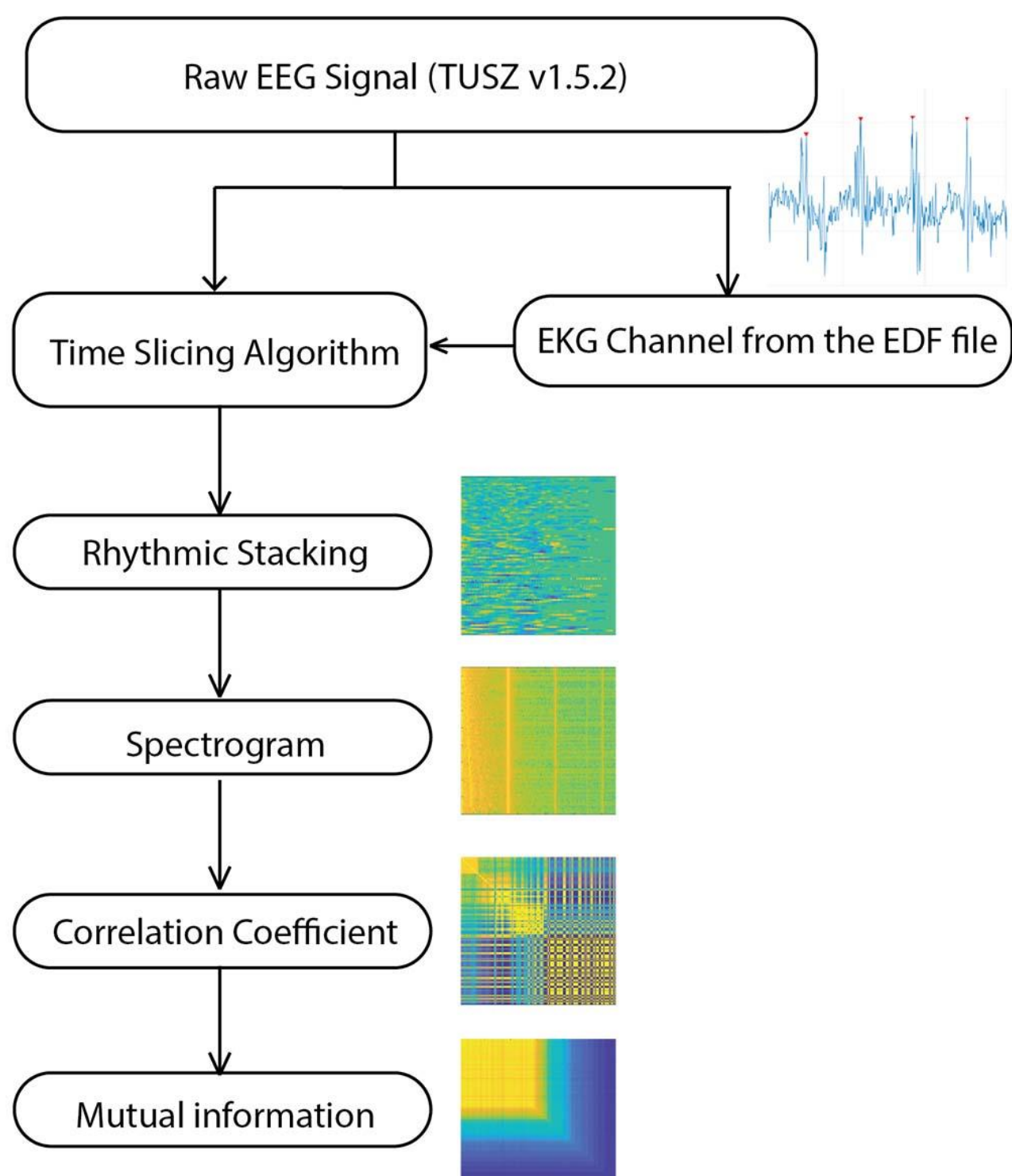


Figure 1 . Steps involved in timeseries to image conversion

SEGMENTATION OF EEG SIGNALS

The underlying principle in this approach is the time-slicing of the EEG recordings based on the R peaks of the ECG signal. The ECG channel is separated by extracting the label EKG-REF or equivalent label from ‘edf’ file. Later the sample index corresponding to ‘r peaks’ was obtained after finding the peaks. Since the time duration of all the channels is the same for one recording, we have sliced the EEG channels based on the ‘r peaks’ of the ECG waveform.

Each such slice is now stacked together to form image data. The slicing procedure and sample of a resultant image is shown in Figure 2. To make the size (width) of the image the same, zero-padded the sequence if there is a mismatch in the length of each segment due to variation in R-R interval. The first algorithm created this image database which is a direct representation of amplitude values in the color-coded form.

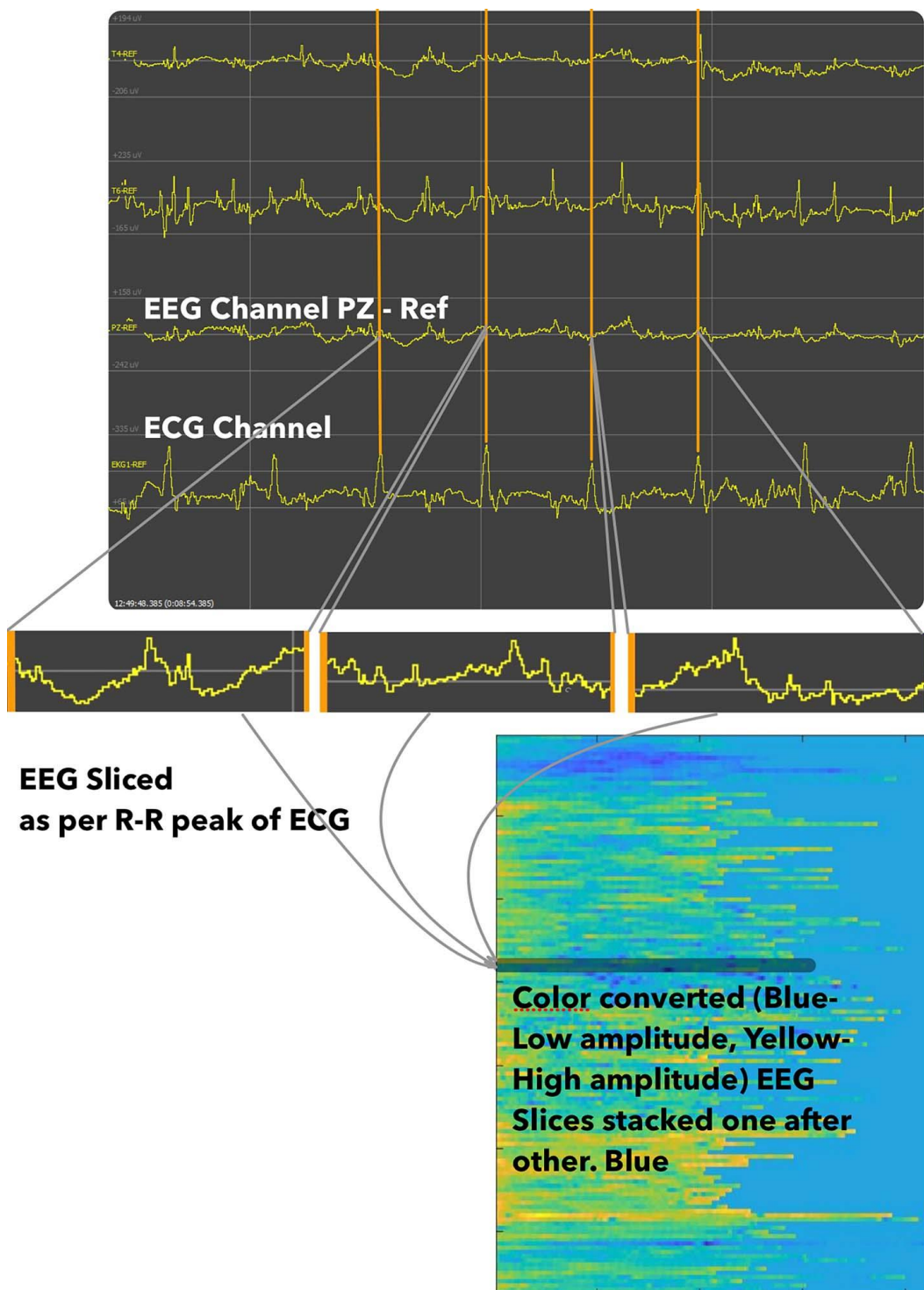


Figure 2. Slicing of EEG based on ECG rhythms

IMAGE CREATION USING SPECTROGRAM, CORRELATION COEFFICIENT AND MUTUAL INFORMATION

In the second algorithm, the entire channel recording without time-slicing is used to obtain the spectrogram images. The spectrogram uses the Short Time Fourier Transform, which is a useful transformation technique since it preserves both time and frequency domain characteristics. The total number of images generated is based on the number of channels available in each ‘edf’ file. In the third algorithm, the correlation coefficient between each time-sliced segment was obtained. Cross-correlation is a technique that estimates the correlation between two signals. Cross-correlation accounts for time delays by shifting one of the two signals. In our approach, the correlation is calculated between two slices, and a matrix is created using the correlation values between each slice. Hence for one channel, if the number of slices is M, we get M correlation coefficient values for each slice.

We get a total of M×M matrix of correlation coefficients. This matrix is further converted to image format. Similarly, in the fourth algorithm, the mutual information between every slice of each channel is obtained. The mutual information matrix corresponds to each channel is converted to images.

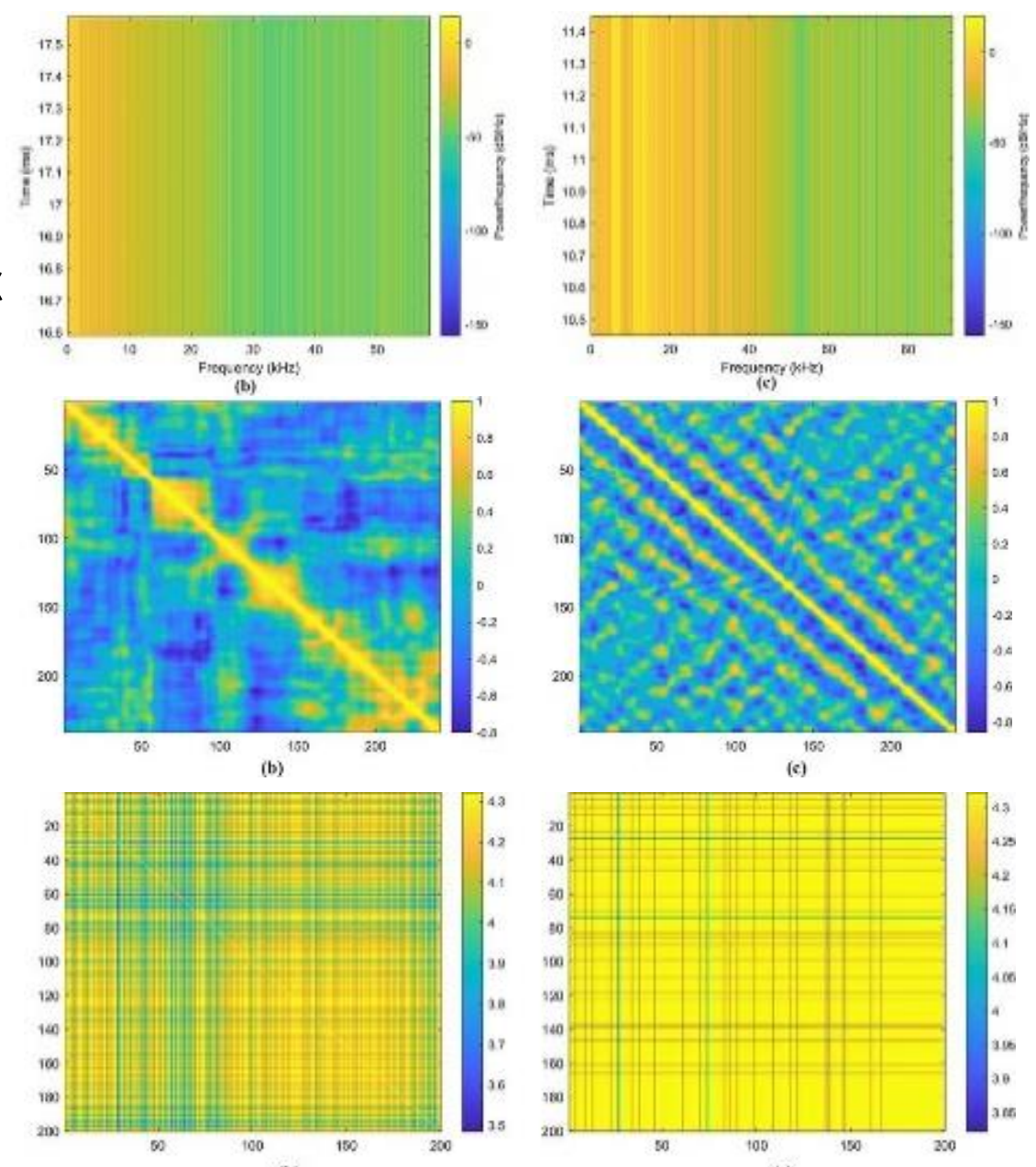


Figure 3 . Sample images generated based on three algorithms

EEG IMAGE DATASTORE

The number of images generated against each category is indicated in the table below. The images created are categorically saved to different folders, corresponding to eight different seizure classes, as shown in Figure 4.

The typical filename of each image is in the format mentioned in Figure 5. The patient number, session ID, and session number fields are the same as in the original EEG file available in the EDF format in the TUSZ database. Using the same naming convention makes it easy for researchers to compare the deep learning algorithms with works that directly use the TUSZ data. The images are cropped to remove the axis information which is generated while implementing the algorithms. Total number of images generated in the current version is listed in Table 1.

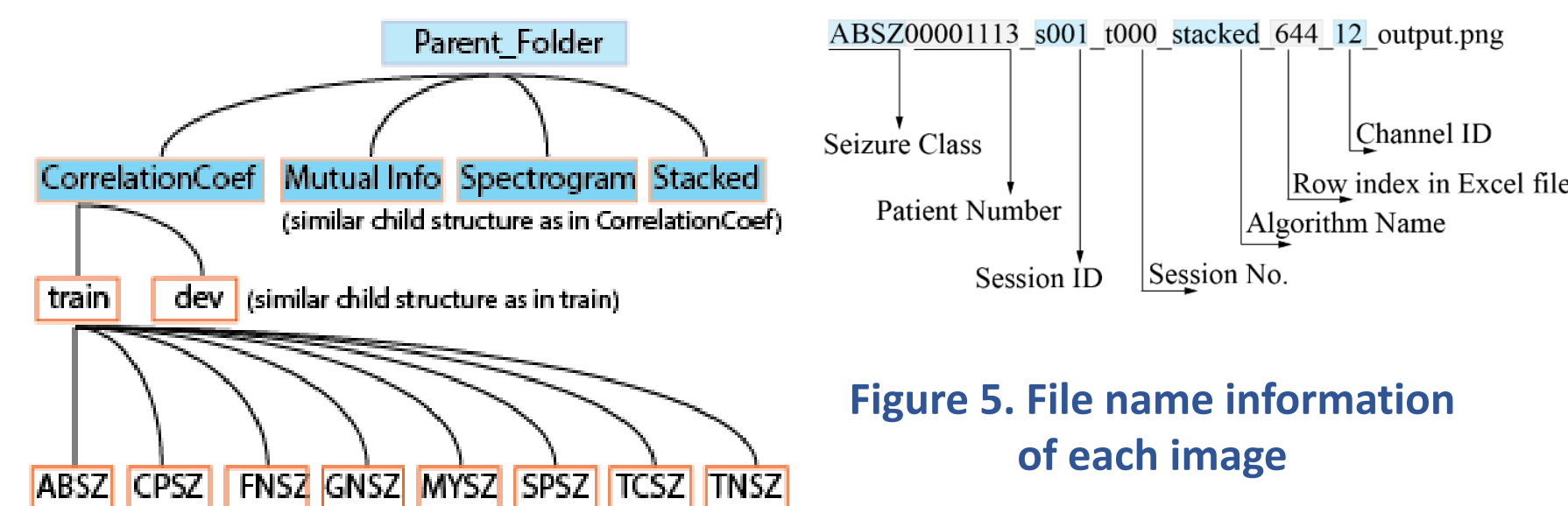


Figure 4. Structure of image folder

	Seizure Category	Stacked images		Spectrogram Images		Correlation based images		Mutual information-based images	
		Train	Dev	Train	Dev	Train	Dev	Train	Dev
		Train	Dev	Train	Dev	Train	Dev	Train	Dev
Image Data Bank 1	FNSZ	26179	2286	42577	4679	2627	1029	232	32
	GNSZ	6415	1644	10964	1592	356	438	121	104
	SPSZ	1179	96	1298	93	151	130	92	34
	CP SZ	4119	256	8797	1111	488	258	164	117
	ABSZ	1056	192	1573	192	84	100	257	111
	TNSZ	279	95	486	589	248	498	215	99
	TCSZ	494	409	900	506	273	348	278	101
	MYSZ	64	32	64	32	64	32	125	10
Image Data Bank 2	Total	39785	5010	66659	8794	4291	2833	1484	608
	FNSZ	1600	1568	672	1568	1582	-	704	-
	GNSZ	7250	2680	6416	2622	3001	-	526	-
	SPSZ	38155	9156	38565	8787	32515	-	950	-
	CP SZ	11199	4880	9052	4751	7741	-	786	-
	ABSZ	64	-	-	32	64	-	64	-
	TNSZ	1462	96	1277	93	1433	-	117	-
	TCSZ	907	550	420	537	907	-	315	-
	MYSZ	540	1408	485	1364	540	-	247	-
	Total	61177	20338	56897	19754	47783	0	3709	0

Table 1. Number of images created under each class of seizure

IMAGE VALIDATION USING CNN

The images were tested for the classification accuracy using three CNN architectures; Alexnet, Resnet18, and GoogleNet. All three pre-trained networks were tuned to match the multiclass requirement (7-Class) by changing parameters in the fully connected layer in each architecture. As indicated in Table 1, the number of images per class is not balanced. This is due to the insufficient recordings available in the corpus for a particular type of seizure (e.g., Myoclonic Seizure). Due to the imbalance in the data, other than validation accuracy, we have calculated F1-Score and Specificity.

The values of training options (hyperparameters) used for training the Alexnet architecture are listed in Table 2. Similar training options were provided for the other two architectures as well.

Solver	sgdm
Initial learning rate	0.0001
Validation frequency	50
Epochs	30
Minimum batch size	128
L ₂ Regularization	0.0001
Gradient Threshold Method	L ₂ Norm
Momentum	0.9

Table 2. Training options

Figure 6 shows the training progress upon training Alexnet architecture with mutual information-based images. The confusion matrix obtained for the same database (mutual information-based images) is shown in Figure 6. Similarly, all four image databases were tested with three CNN architectures.

RESULTS AND DISCUSSIONS

Figure 6 shows the training progress upon training Alexnet architecture with mutual information-based images. The confusion matrix obtained for the same database (mutual information-based images) is shown in Figure 6. Similarly, all four image databases were tested with three CNN architectures.

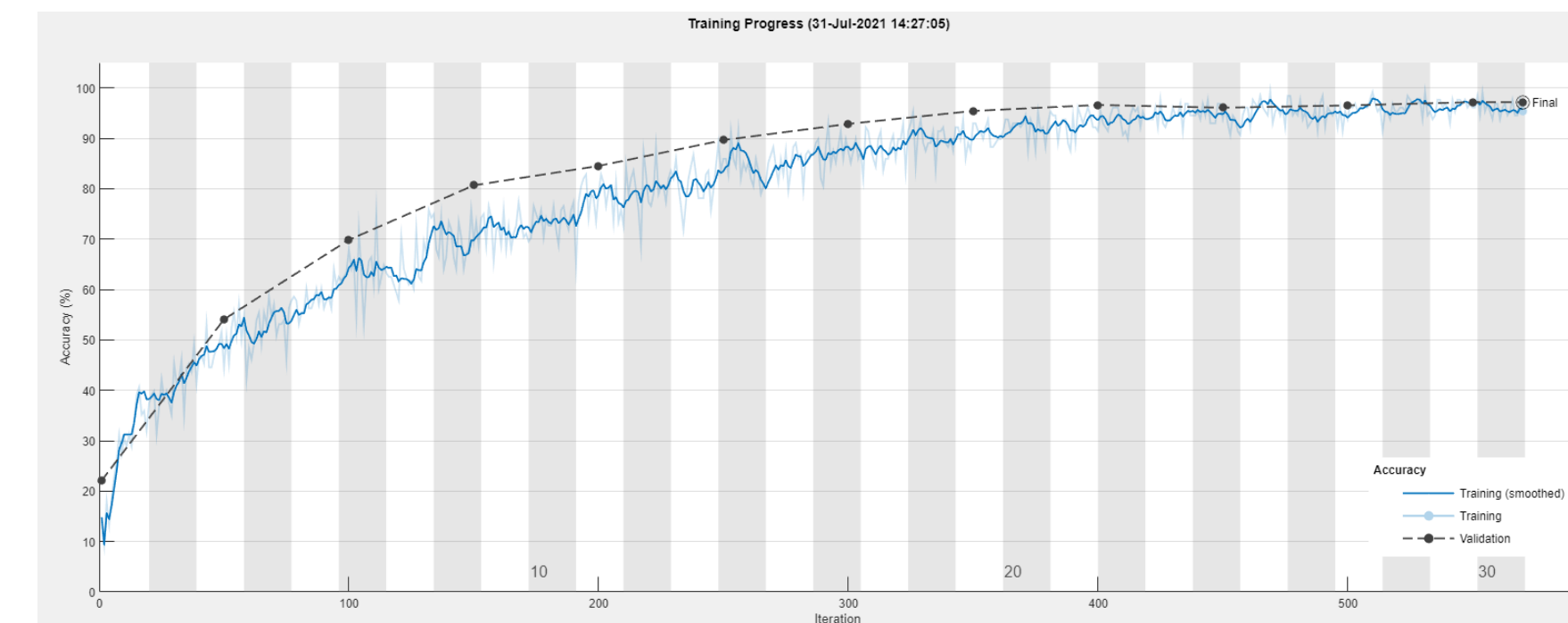


Figure 6. Training Progress of mutual information-based images with AlexNet architecture

Confusion Matrix												
Output Class	ABSZ	CP SZ	FNSZ	GNSZ	SPSZ	TCSZ	TNSZ	Accuracy				
	207 19.0%	1 0.1%	0 0.0%	0 0.1%	0 0.0%	0 0.0%	0 0.0%	99.0%	1.0%			
	0 0.0%	153 14.0%	1 0.1%	0 0.0%	0 0.0%	0 0.0%	0 0.0%	99.4%	0.6%			
	0 0.0%	0 0.0%	277 25.4%	6 0.5%	0 0.0%	0 0.0%	2 0.2%	97.2%	2.8%			
	4 0.4%	3 0.3%	4 0.4%	229 21.0%	0 0.0%	0 0.0%	0 0.0%	95.4%	4.6%			
	0 0.0%	0 0.0%	0 0.0%	0 0.0%	33 3.0%	1 0.1%	0 0.0%	97.1%	2.9%			
	0 0.0%	1 0.1%	1 0.1%	0 0.0%	0 0.0%	91 8.3%	0 0.0%	97.8%	2.2%			
	0 0.0%	0 0.0%	2 0.2%	0 0.0%	2 0.2%	2 0.2%	70 6.4%	92.1%	7.9%			
								Target Class	Accuracy	Specificity	F1 - Score	F2 - Score

Figure 6. Confusion Matrix

The performance of our approach is compared with similar works performed on the TUH database by other authors. Golmohammadi et al. used GRU and LSTM models on TUH Seizure data and achieved a specificity of 97.1 % and 91.49 %. L. Wei and A. Mooney presented the XGBoost-based method to detect seizures from TUH Corpus and achieved an accuracy of 67.01% while training and 58.85% during validation. For the abnormal dataset from the TUH EEG corpus, S Roy et al. applied 1D-CNN-RNN and could achieve an accuracy of 82.27%. Yildirim et al. proposed a 1D CNN model to classify the normal and abnormal EEG signal from the TUH EEG corpus and achieved an F1-Score of 78.92 and an accuracy of 79.34%.

Spectrogram Images (AlexNet)	F1 - Score	97.47
	Accuracy	97.15
	Specificity	99.51
Correlation Coefficient based Images (ResNet-18)	F1 - Score	93.64
	Accuracy	93.45
	Specificity	98.88
Mutual information based Images (ResNet-18)	F1 - Score	97.95
	Accuracy	97.89
	Specificity	99.62
Stacked Images (ResNet-18)	F1 - Score	95.64
	Accuracy	95.50
	Specificity	99.24

Table 3. Summary of performance parameters

CONCLUSION

In this abstract, we have discussed the generation of an image database from TUSZ v1.5.2 using four techniques. The images are tested for classification accuracy using CNN. The highest accuracy of 97.89% has been achieved when trained ResNet architecture with images based on mutual information. The accuracy achieved is for seven classes. The image database serves as a valuable resource for training deep learning networks.

ACKNOWLEDGEMENT

This research is supported by the research laboratory of the ECE department at BMS Institute of Technology and Management. The database used in this work is provided by The Neural Engineering Data Consortium (NEDC) at Temple University.